Climate Dynamics (2002) 19: 599–608
DOI 10.1007/s00382-002-0247-7

J.C. Rogers · M.J. McHugh

On the separability of the North Atlantic oscillation and Arctic oscillation

Received: 13 July 2001 / Accepted: 30 January 2002 / Published online: 28 May 2002

Abstract We address the issue of whether the Arctic (AO), and North Atlantic oscillations (NAO) are inseparable, forming an annular mode in the Northern Hemisphere atmospheric circulation. This annular mode is the leading empirical orthogonal function of hemispheric sea level pressure (SLP) data, explaining the largest amount of its variability. We examine whether the NAO and AO are inseparable spatial modes of the atmospheric circulation using rotated principal component analysis (RPCA), a methodology that identifies simple and unique patterns of spatial dataset variability. RPCA of the spring, summer, and autumn SLP fields from 1946–1998 reveal NAO and AO-like patterns, occurring as separate regional teleconnections forming the first and second principal components respectively. The RPCA-based NAO dipole pattern is like that observed in many prior studies, while the AO-like pattern exhibits high SLP variability over the Kara and Laptev seas. During winter however, and in annual analyses, a distinct AO-like pattern is not obtained and the two patterns may be inseparable using commonly accepted RPCA methods. The RPCA-based AO-like mode is significantly linked to north-central Siberian seasonal air temperatures and to the prevailing direction of motion of the underlying Arctic Ocean in summer, suggesting that the non-winter AO-like pattern, as a stand alone teleconnection separate from the NAO, contributes significantly to high-latitude climate and ocean variability. The winter NAO/AO inseparability is discussed as a possible effect of a shared winter storm track between the northeastern Atlantic and the Arctic.

J.C. Rogers (✉)
Department of Geography and Atmospheric Sciences Program, Ohio State University, Columbus, OH 43210-1361, USA
E-mail: rogers.21@osu.edu

M.J. McHugh
Department of Geography, University of Wisconsin – Oshkosh, Oshkosh, WI 54901-8642, USA

1 Introduction

The low frequency (monthly time scales) component of atmospheric circulation variability has been widely examined over the last 30 years. An outcome of many studies has been the characterization of atmospheric teleconnections, spatial patterns of atmospheric low-frequency circulation covariability between widely separated points around the globe. The component patterns of atmospheric circulation have been identified using either (1) correlation methods (Walker and Bliss 1932; Wallace and Gutzler 1981) or (2) forms of eigenvector methodologies that help reduce large datasets to their primary modes of variability. Eigenvector methods typically include the use of principal component analysis (PCA; Kutzbach 1967; Barnston and Livezey 1987; Rogers 1990) but methods such as combined (Bretherton et al. 1992) and complex (Horel 1984) PCA, singular value decomposition (Wallace et al. 1992), and canonical correlation analysis (e.g., Nicholls 1987; Metz 1989) are widely used. More recently, methods such as non-linear PCA have come into use (Monahan 2000; Monahan et al. 2001).

There are methodological differences among PCA studies, often based around the question of whether to apply orthogonal or oblique rotation to the unrotated eigenvector fields. In unrotated analyses the first eigenvector, or empirical orthogonal function (EOF), accounts for the largest amount of overall dataset variance. Walsh and Richman (1981, their Appendix) state that ''while the maximization of variance may be desirable in some applications, it may be achieved at the expense of the representativeness of the computed patterns.'' The major advantage of eigenvector rotation is to obtain a more accurate representation of the dominant spatial modes of the data fields than occurs in the unrotated solutions, although it is achieved by a redistribution of the dataset variance contained in the first few unrotated EOFs. Walsh and Richman (1981) point

out that the variance redistribution occurring with rotation can be disadvantageous, although generally only if the variance is *highly concentrated* in the first one or two unrotated modes, in which case rotation may in fact dilute the variance content of the unrotated modes and no single rotated mode will then provide a useful measure of the dataset variances. Unrotated analyses pertinent to this study include Kutzbach (1970), Trenberth and Paolino (1981) and Thompson and Wallace (1998, 2000). Studies employing orthogonal rotation of the principal components in their analytical solution include (for example) Horel (1981), Hsu and Wallace (1985), Barnston and Livezey (1987), Kushnir and Wallace (1989) and Rogers (1990).

Walker and Bliss's (1932) correlation work in the 1920s identified sea level pressure (SLP) teleconnection patterns such as the North Atlantic Oscillation (NAO) and Southern Oscillation. The NAO also appears as the leading mode in PCAs of SLP and 700 hPa heights having a 20°–70°N latitude dataset domain limit (Kutzbach 1970; Barnston and Livezey 1987; Rogers 1990). It appears spatially as an atmospheric mass oscillation between the subpolar northern Atlantic and the lower midlatitudes and subtropics of that ocean, and environs, occurring in all months of the year. At 500 hPa the NAO begins to take on the characteristics of its thermal response, exhibiting characteristic spatial centers of action over Greenland and northern Europe (van Loon and Rogers 1978; Wallace and Gutzler 1981).

The Arctic Oscillation (AO) has recently been identified (Thompson and Wallace, 1998; hereafter TW98) as a unique teleconnection pattern, named in accordance with the historical precedent of Walker and Bliss (Wallace 2000). The AO is the leading surface EOF (TW98), explaining the greatest amount of dataset variance in their November–April (TW98) and a 12-month combined analysis (Thompson and Wallace 2000) covering 1958–1997. It is characterized by a seesaw in atmospheric mass between the Arctic and mid-latitudes, comprised of both a zonally symmetric equivalent barotropic structure, extending into the stratosphere, and a wave-like baroclinic signature in the troposphere. The leading EOF's spatial form incorporates the Atlantic sector NAO but has little correlation in the Pacific sector (Deser 2000). For example, the main area of Arctic pressure variability extends southward into the area around Greenland and Iceland and the opposing mid-latitude pressure center is a broad area focused around the subtropical Atlantic. The AO is also apparent in seasonal Arctic-inclusive unrotated SLP analyses (Trenberth and Paolino 1981) where it is the first EOF in all seasons except autumn (when it was the second EOF).

Thompson and Wallace (2000) show the similarities between the AO and a pronounced zonally symmetric pressure field variability pattern in the Southern Hemisphere. Together, they refer to the zonally symmetric hemispheric pressure field patterns centered on the Arctic Ocean and Antarctica as "annular modes". Wallace (2000) furthermore advocates that the NAO and AO are inseparable, forming the Northern Hemisphere annular mode. He argues that the NAO is only distinctly separate from the annular mode when narrowly defined in terms of simple station-based pressure indices (e.g., Azore/Iceland pressure differences). Instead the NAO/AO annular mode is a pattern that explains the largest amount of the Northern Hemisphere dataset variance and it has a basis in the concepts of the zonal wind index (Namias 1950) and polar pressure deficit (Gates 1950).

The purpose here is to quantitatively evaluate the notion of the inseparability of the NAO and AO in an annular mode of the Northern Hemisphere. We will use the same dataset as in TW98 with the exception of using traditional seasons (DJF, MAM, JJA, SON) and an orthogonally rotated principal component analysis (RPCA). Our objective in using RPCA is to focus on the dominant spatial modes of pressure variability in a dataset extending to the pole. We also briefly examine how the rotated components are linked to some elements of high latitude climate fields and ocean circulation. The Southern Hemisphere is not analyzed here as its annular mode has already been identified using RPCA (Rogers and van Loon 1982).

2 Data and methodology

Monthly mean SLPs are used, extending from 1946–1998 and available on a 5° × 5° grid from 20° to 85°N. The data, available from the NCAR data support section, have been tested and adjusted for errors (Trenberth and Paolino 1980) and were also used in Thompson and Wallace's (1998, 2000) analyses. Based on daily weather maps, the SLPs are complete to 85°N, unlike pre-1946 data in which pressure values along 75°N and 85°N, or over Asia are often missing. Any undetected small-scale errors in the dataset will be isolated by the principal component procedure and relegated to the smaller eigenvectors that are not retained here for rotation. The final analysis fields consist of a 5° latitude by 20° longitude subset grid extending from 30°N to 85°N. Data are transformed into departures from the 52-year normal of each individual month and adjusted by the cosine of latitude so as to reduce the impact of higher variance with increasing latitude. Alternating longitudinal grid points were removed from the data between 75°N and 85°N to lessen the density of grid points at higher latitudes due to the convergence of meridians. RPCA was performed on the seasonal three-month groups, and on an annual analysis that incorporated all data sequentially from March 1946 through February 1998.

The first unrotated eigenvector maximizes the variance explained in the dataset and in that context has potential physical meaning (Richman 1987). The same however is not true of the subsequent patterns and in general the unrotated solutions seldom show the simple, unique, statistically robust patterns of spatial variability taking place in the dataset (Richman 1986). In order to obtain statistically robust patterns, orthogonal rotation is performed on a certain number of the unrotated patterns, using the varimax procedure. As in Rogers (1990), the decision regarding how many patterns to retain for rotation is based on scree plots of the eigenvalues. In making the decision, we identify the location of the first major "shelf" in the eigenvalues (O'Lenic and Livezey 1988), wherein the final "shelf" eigenvalue still accounts for more than 5% of the total unrotated dataset variance. RPCA methodology retains between five and seven factors for rotation in the individual seasonal and annual analyses performed here (Table 1). This is fairly typical, many studies retain about a half-dozen factors

Table 1. Basic characteristics of the seasonal unrotated eigenvector analyses, including the variance explained by EOFs 1 and 2 and the number of factors retained for orthogonal rotation. Coefficients of correlation are calculated between seasonal unrotated scores obtained here and seasonally averaged TW98 scores based on the TREN/NCEP dataset

Season:	Spring	Summer	Autumn	Winter	Annual
Correlation with TW98	–0.99	–0.96	–0.76	–0.99	NA
EOF 1 variance	24.0%	17.9%	14.3%	23.2%	20.0%
EOF 2 variance	10.4%	8.2%	13.6%	13.1%	10.3%
Factors retained	6	5	7	6	7

for rotation. At the higher end, Barnston and Livezey (1987) required that ten components be retained in each monthly analysis and Rogers (1990) retained between eight and 11.

RPCA produces spatial patterns or loading vectors that give the amplitude and polarity of a given principal component at each grid point. Component "scores" yield the temporal variability of either the unrotated or rotated components. The scores have a mean of zero and the components remain collectively uncorrelated with each other when orthogonal rotation is performed. The original spatial loading vectors are not presented in the results, in favor of pressure field patterns obtained as follows. In each month we identify the six highest and six lowest scores, yielding 18 case/months per meteorological season of each sign. The seasonal mean pressure for both the positive and negative modes is determined and the mean SLP difference between them is obtained and tested for statistical significance using a two-tailed t-test. Differences achieving statistical significance generally always correspond to grid points with the highest loading values in the original RPCA, and they are the focus of our results. For the sake of brevity, the complete set of seasonal RPCA-based composite maps are not presented, focusing rather on the components representing the NAO and AO.

In making comparisons to TW98, we use their NAO/AO annular mode time series available at http://www.atmos.colostate.edu/ao/Data/ao_index.html, that is based on the EOFs of the "TREN/NCEP" dataset comprised of Trenberth and Paolino's (1981) SLPs through 1957 and subsequently by NCEP reanalyses. These will be referred to as the TW98 time series. Time series are also used of the basic NAO index (NAOI) defined by the pressure difference between Ponta Delgada, Azores, and Akureyri, Iceland (Rogers 1984) updated on http://www-bprc.mps.ohio-state.edu/NAO/index.html.

3 Results

Initially, unrotated principal components were obtained for each season. In all seasons the first two EOFs explain under 40% of the dataset variance (Table 1). The time series scores of the unrotated seasonal analyses obtained here are compared to seasonally-stratified monthly time series scores from TW98. Results (Table 1) reveal very high, significant, correlations in all seasons with coefficients between the two dataset time series exceeding $r = 0.96$ ($n = 156$) in winter, spring and summer. The autumn variance of our unrotated Arctic SLP field is spread over the first two unrotated components, each of which equally accounts for about 14% of the seasonal dataset variance (Table 1). Nonetheless, the correlation between the leading EOF and TW98s autumn time series still has a sizeable coefficient of variation above 50%. The correlations in Table 1 suggest that TW98s eigenvector analysis has been reasonably well reproduced here even though we (1) stratified our data seasonally, (2) used dissimilar techniques to reduce the number of high-latitude grid points, and (3) TW98 included data from 1899–1945. The remainder of this section presents the RPC and associated analyses.

3.1 Non-winter seasons

A classic NAO SLP pattern is the first rotated component of the spring SLP field (Fig. 1a), characterized by

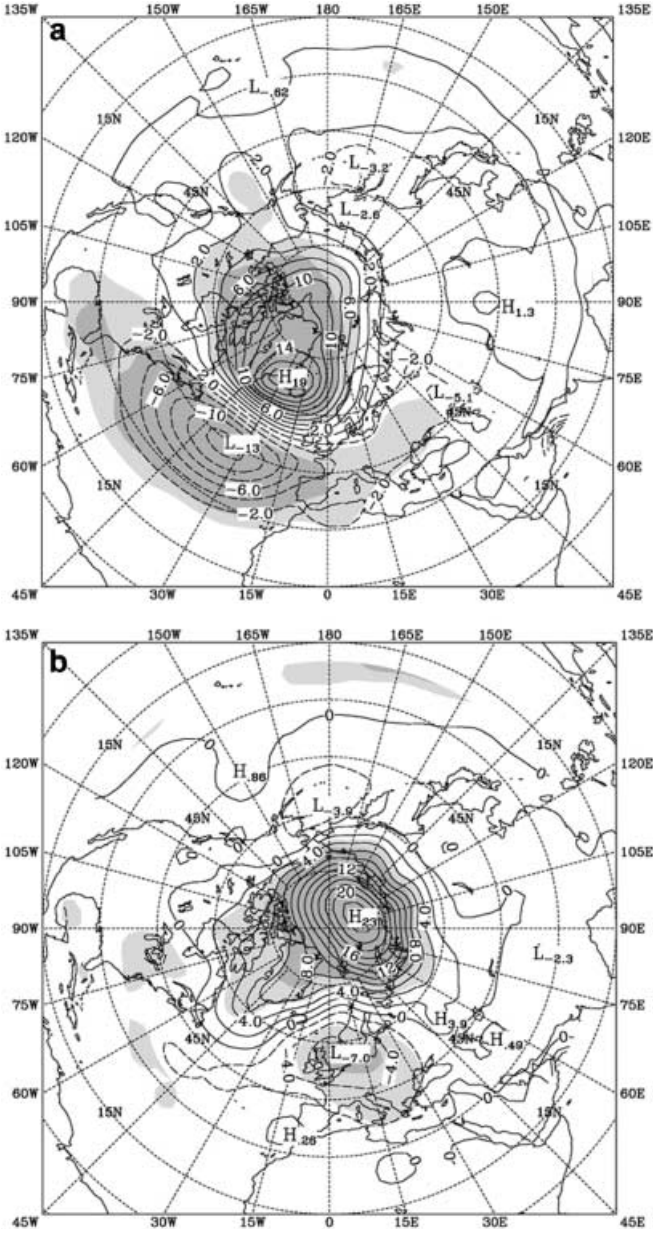

Fig. 1a,b. Mean spring sea level pressure differences (hpa) between seasons with highest mean positive and mean negative time series of (a) RPCA one (NAO) and (b) RPCA two (AO-like mode). Shaded areas represent pressure differences that are statistically non-zero with 95% and 99% confidence

an Atlantic pressure dipole with centers over the Denmark Strait, between Greenland and Iceland, and broadly across the central Atlantic with a maximum near 45°N, 35°W. Arctic pressure differences are significantly high throughout northernmost Canada and the Canadian Basin of the Arctic Ocean, while lower latitude pressure differences achieve 95% significance into central Europe and the eastern United States.

The second rotated spring component exhibits a large 23 hPa pressure difference over the Laptev Sea of the Arctic Ocean. This AO-like pattern contains significant Arctic basin pressure differences opposite those of continental mid-latitudes, but little significant pressure difference near the Iceland and Azores NAO centers. Arctic SLP differences exceeding 95% significance in components 1 and 2 overlap over the Canadian sector of the Arctic Ocean and northern Canada, south of the Great Lakes, and in central Europe. The implied overlap in the spatial loadings in some areas is not unexpected since only the temporal series are orthogonalized by rotation.

Summer component 1 is characterized by a somewhat less expansive NAO compared to spring, especially in lower latitudes where the central Atlantic pressure differences do not reach 5 hPa (Fig. 2a). The Arctic center lies across Greenland and again extends across northernmost Canada and the Canadian Basin. The AO-like component (Fig. 2b), is also centered again over the Arctic Ocean basin, tending toward the Laptev Sea. The summer AO pattern exhibits an extensive dipole structure of significant pressure differences between the Arctic and mid-latitudes, especially eastern Asia and North America.

The subpolar center of the NAO returns to the Denmark Strait (Fig. 3a) in autumn, while a very broad band of significant pressure differences of opposite sign lies across the mid-latitudes from central North America, across the Atlantic to central Europe. The autumn AO-like component (Fig. 3b), is centered across the Kara and Laptev seas, much closer to the coast than in summer, and extends across eastern Siberia toward the Kamchatka Peninsula. The dipolar AO structure is weaker than that prevailing across the hemisphere in the NAO component.

Figure 4a–d provides a representative example, from spring, of the mean SLP fields during positive or negative phases in the non-winter seasons. The sign of the NAO is reversed in this analysis from its normal usage (e.g., positive mode usually corresponds to strong Atlantic westerlies). The NAO positive mode (Fig. 4a) is dominated by high pressure over the Canadian Arctic and Greenland, providing a sizeable area where surface polar easterlies may dominate the flow. The ''Icelandic low'' lies east of Newfoundland. The NAO negative mode (Fig. 4b) exhibits a deep Icelandic low anchored in the Denmark Strait with a northeastward extended trough into the Arctic Basin and a northward displaced Atlantic pressure gradient. The AO positive mode (Fig. 4c) is characterized by high pressure exceeding

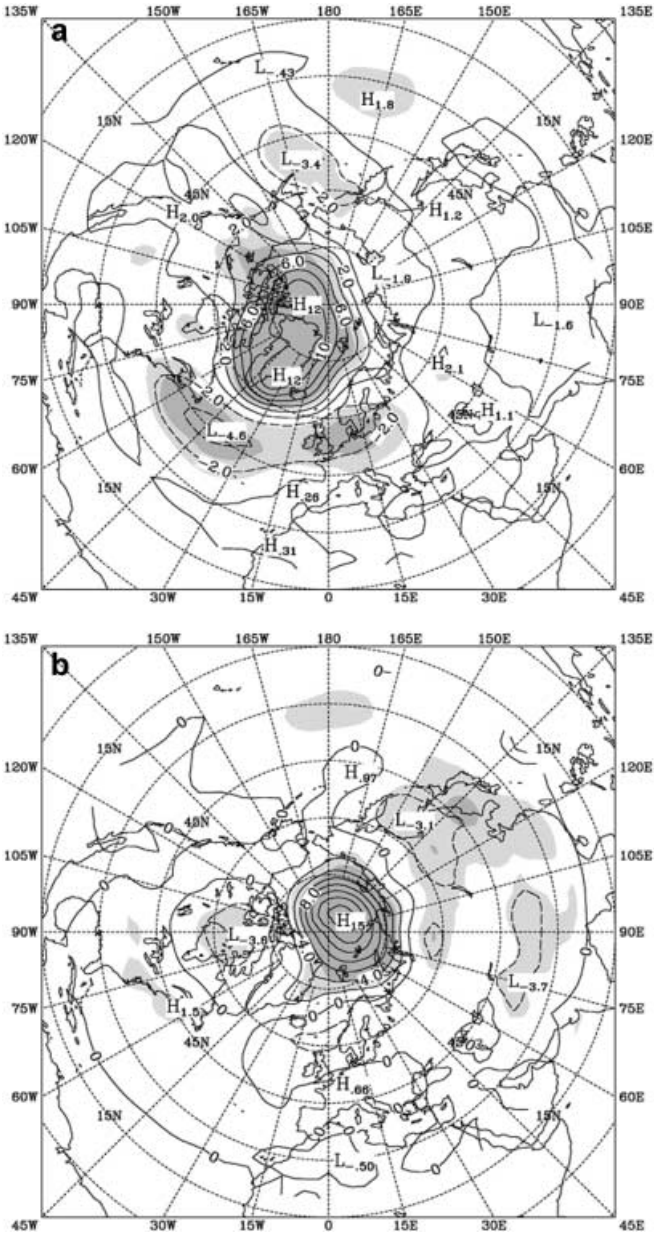

Fig. 2a,b. Same as Figure 1 but for summer

1030 hPa in the Laptev Sea, a weak northern Atlantic pressure gradient, and a subpolar low lying over the Norwegian Sea. The AO negative mode (Fig. 4d) exhibits broad low pressure, under 1008 hPa, extending along the Eurasian coastline from the Barents to the Laptev Sea. A trough of low pressure extends southwestward toward the Denmark Strait.

Seasonally averaged time series of TW98s NAO/AO annular mode are correlated (Table 2) to the non-winter seasonal scores of both the first and second rotated components presented in Figs. 1–3. RPCA time series are significantly correlated to TW98s series although the coefficients are not as high as in the unrotated comparison analyses in Table 1. Component one (NAO) scores have higher coefficients than those of component two

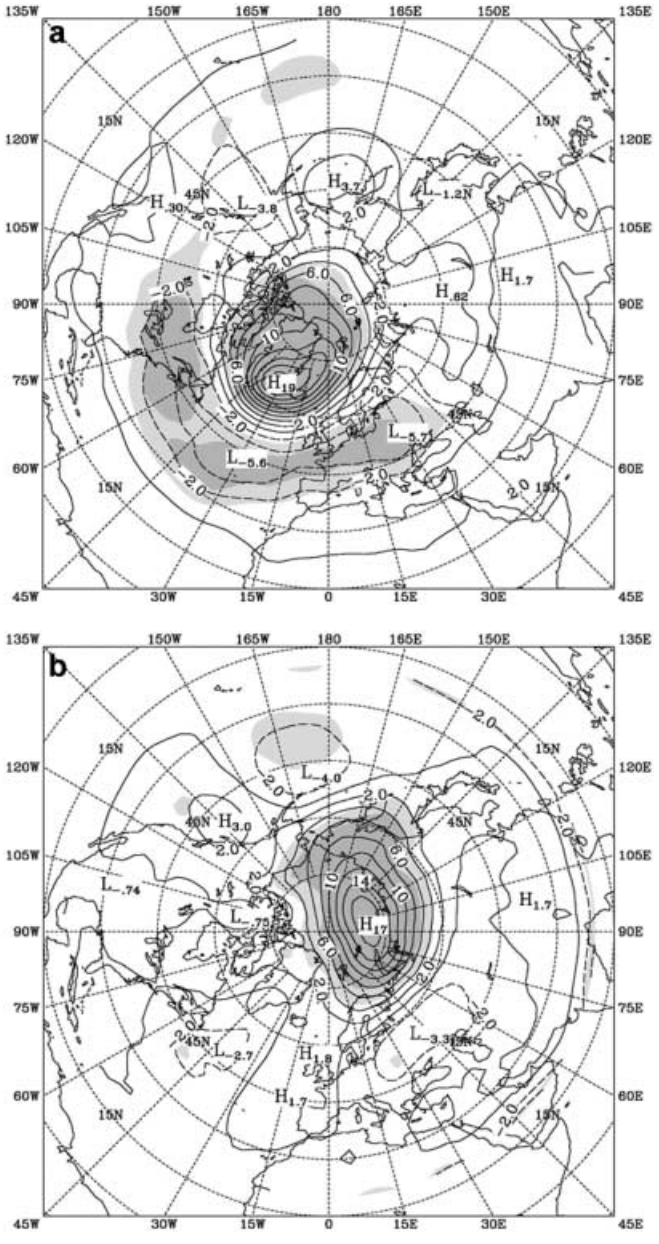

Fig. 3a,b. Same as Figure 1 but for autumn

(AO) to the TW98 series. The station-based NAOI is, not unexpectedly, highly correlated to RPCA 1 scores, but not those of RPCA 2, and it also has high correlation to the TW98 time series scores. The results of Table 2 provide some indication of the strong link of TW98s series to the NAO while in contrast the AO-like RPCA signal (component 2) found here is not as well correlated to TW98 and is dissociated from the NAOI.

3.2 Winter, and the annual analysis

The first principal component of the winter SLP fields (Fig. 5) exhibits a large dipole between the Arctic Ocean, Greenland, and Iceland region and the subtropical Atlantic and Mediterranean basin. The analysis does not produce a separate AO-like pattern, as in Figs. 1b–3b. Figure 5 bears only a partial resemblance to TW98s annular mode (their Fig. 2), lacking both zonally symmetric structure and significant pressure responses over central Eurasia and the northern Pacific. The pattern instead resembles that of the spring NAO (Fig. 1a) except for the presence of a small east-Asian center which, in spring, appears as part of the AO-like pattern (Fig. 1b). Pressure differences that have been part of the AO-like patterns (Fig. 1b–3b) on the Eurasian side of the Arctic Ocean basin are confined in winter to the periphery of rotated patterns two and three, exhibiting centers over Siberia and the Aleutians, respectively (not shown). This result remains unchanged even when as many as 11 components are retained for rotation, a number that methodologically is the upper limit for this type of dataset.

An annual analysis was performed that included all data from March 1946 through February 1998, retaining seven components for rotation. The pressure differences linked with this component are very similar to those obtained for the winter analysis (Fig. 5) and are not shown. A broad mid-latitude region of statistical significance again lies across the Atlantic and Europe with a sign opposite that of the polar region with the polar center extending into the northern Atlantic across Greenland and Iceland. When eleven components are retained for rotation in the annual analysis, the pattern reverts to that of the non-winter seasons with distinct AO- and NAO-like patterns, although the former becomes the primary component while the NAO is the second component. Retaining 11 patterns violates some basic tenets however. Components 10 and 11 comprise the second ledge of the scree plot and patterns beyond number seven account for less than 5% of the dataset variance and would ordinarily not be included in such an analysis.

3.3 Correlations to high latitude climate data

TW98 performed a series of correlations between their annular NAO/AO pattern time series and other climatic series such as Eurasian air temperatures and stratospheric 50 hPa geopotential heights. Similar analyses are performed here (Table 3) to show the comparative correlations between TW98s time series and the RPCA scores. The comparative analyses in Table 3 include (1) Eurasian air temperatures (40°–70°N, 0°–140°E), as in TW98, (2) Siberian air temperatures over a subregion of Eurasia (65°–80°N, 80°E–140°E), and (3) stratospheric 50 hPa geopotential heights at grid points located close to rawinsonde stations on northern Asia (75°N, 105°E) and northwestern Greenland (80°N, 60°W) and located on opposite sides of a large area of high polar stratospheric response to the NAO/AO mode (TW98; their Fig. 1). The Siberian region temperatures (2) are chosen as a potential ''best-case'' scenario since this region is

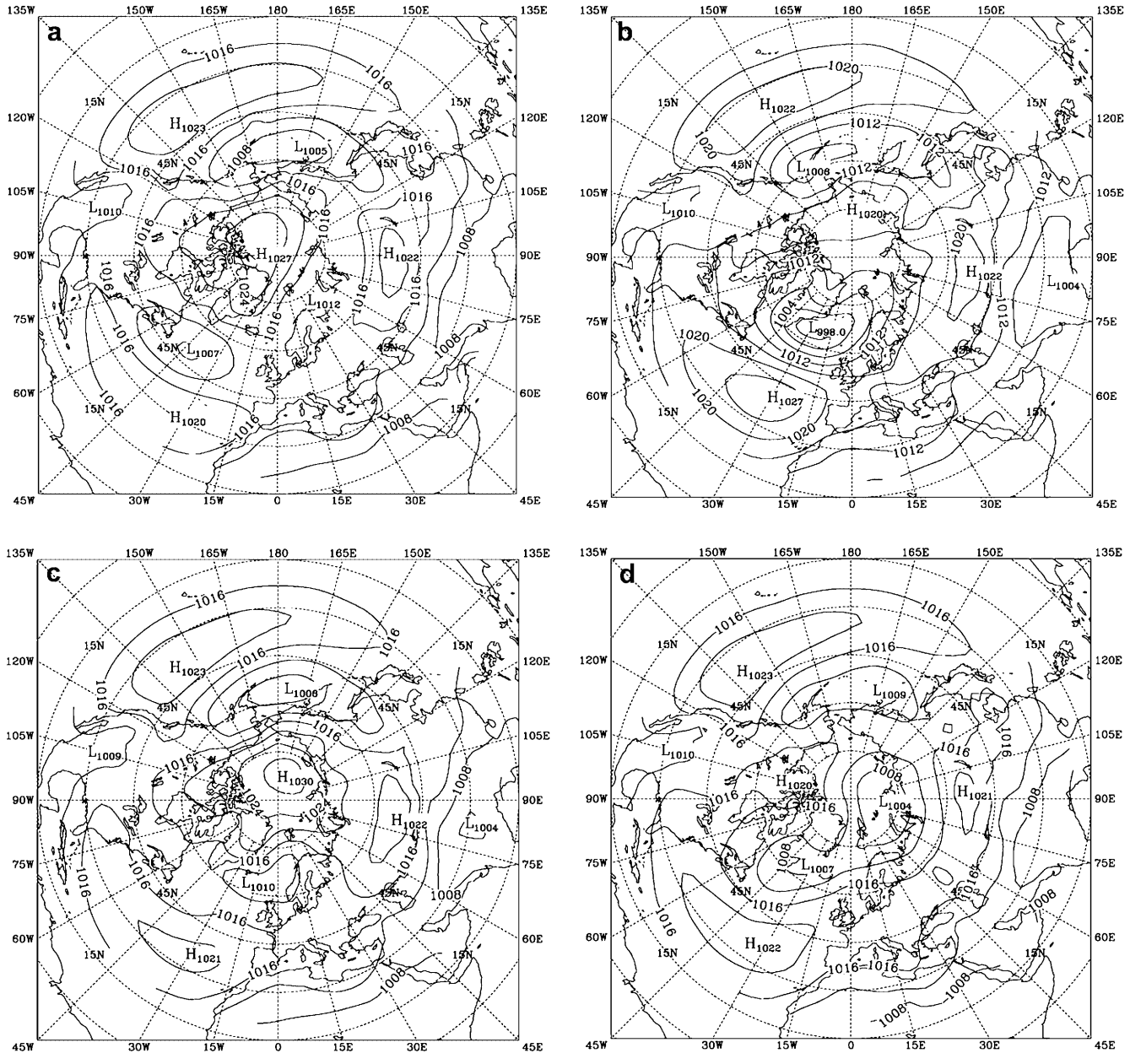

Fig. 4a–d. Spring seasonal mean sea level pressure (hPa) for the (**a**) positive and (**b**) negative modes of the NAO (RPCA 1) and (**c**) positive and (**d**) negative modes of the AO-like pattern (RPCA 2)

closer to the Kara Sea area of highest pressure response in our rotated AO-like modes in Fig. 1–3. Winter temperatures in north-central Siberia have also been linked to interannual variability of Arctic basin cyclonic activity (Rogers and Mosley-Thompson 1995). Data for these analyses are gridded monthly mean NCEP/NCAR reanalyses available for 1949–1998.

Throughout Table 3, correlation coefficients are generally significantly non-zero with more that 95% confidence in all seasons but summer. Correlation coefficients between TW98s time series and winter and spring Eurasian temperatures exceed those of the AO-like RPCA scores but they are slightly lower in absolute magnitude in summer and autumn. The AO-like RPCA coefficients match or slightly exceed those of TW98 for the north-central Siberian temperatures. RPCA 1 scores

Table 2. Seasonal correlations between RPCA-based NAO and AO time series, the station-based NAO index, and TW98s dataset time series scores based on the TREN/NCEP SLPs. Winter correlations are based on EOF 1 scores (Fig. 5) only. Correlations above absolute $r = 0.50$ are significant with 99.9% confidence ($n = 52$)

	Spring	Summer	Autumn	Winter
RPCA 1 versus TW98	–0.71	–0.81	–0.65	–0.84
RPCA 2 versus TW98	–0.64	–0.49	–0.55	–0.84
NAOI versus TW98	0.73	0.64	0.48	0.82
RPCA 1 versus NAOI	–0.93	–0.71	–0.79	–0.74
RPCA 2 versus NAOI	–0.13	–0.18	+0.06	–0.74

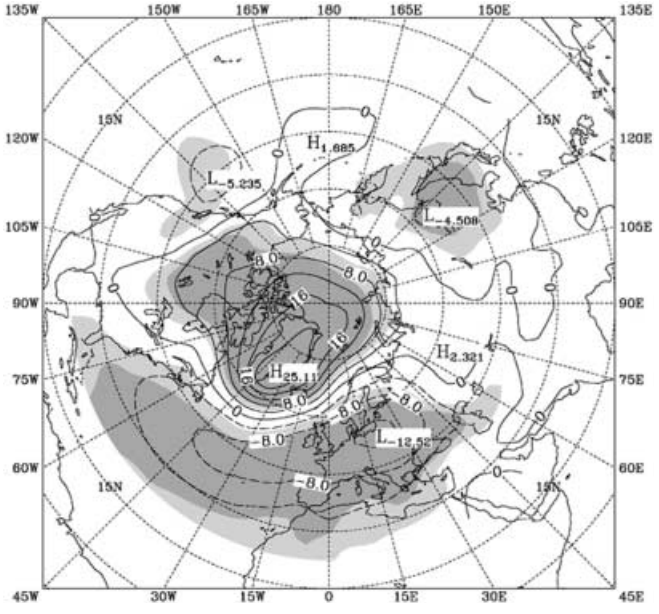

Fig. 5. Mean winter sea level pressure differences (hpa) for years with highest mean positive and mean negative time series of RPCA one. Shaded areas represent pressure differences that are statistically non-zero with 95% and 99% confidence

Table 3. Seasonal correlations of Eurasian air temperatures and stratospheric heights with RPCA scores and TW98s seasonal scores. In all cases the winter AO coefficient is EOF 1. The 95%, 99% and 99.9% confidence intervals occur with absolute coefficients of $r = 0.29$, $r = 0.37$, $r = 0.52$ ($n = 49$)

	Spring	Summer	Autumn	Winter
Eurasian temperatures				
TW98	+0.58	+0.20	+0.46	+0.72
AO RPCA EOF2	–0.48	–0.24	–0.53	–0.49
Siberian temperature				
TW98	+0.46	+0.02	+0.54	+0.57
AO RPCA EOF2	–0.58	–0.03	–0.54	–0.61
50 hPa heights Siberia				
TW98	–0.52	–0.25	–0.35	–0.61
AO RPCA EOF2	0.57	0.32	0.37	0.48
50 hPa heights Greenland				
TW98	–0.39	–0.47	–0.73	–0.62
AO RPCA EOF2	0.38	0.27	0.40	0.64
NAO RPCA EOF1	0.15	0.38	0.52	0.64

Table 4. The mean values and standard deviations (in parentheses) of the RPCA 2 (AO-like pattern) and TW98s unrotated time series during summers when the Arctic Ocean exhibited anticyclonic and cyclonic circulation (Proshutinsky and Johnson 1997). *T*-test values above absolute 2.0 (3.3) are significantly non-zero with 95% (99.9%) confidence

	Anticyclonic ocean	Cyclonic ocean	*t*-test value
AO RPCA EOF 2	+0.41 (0.52)	–0.41 (0.68)	+4.9
TW98	–0.046 (0.313)	+0.148 (0.341)	–2.1

(NAO) are consistently non-significant (and are not shown here), suggesting with TW98 that the NAO exhibits little covariability with Eurasian or Siberian air temperatures. The RPCA AO component correlations to non-winter 50 hPa heights exceed those for TW98s at the Siberian point near the RPCA-based AO's Arctic basin SLP variability maximum. At point 2 near Greenland however, the RPCA AO coefficients are exceeded by those of component one (NAO) in summer and autumn but neither exceeds those of TW98 in non-winter seasons. The results of Table 3 show that the individual RPCA-based NAO and AO time series have correlations to elements of the climate and general circulation comparable to those of TW98s series, designed to produce a mode that maximized SLP dataset variance.

While summer season produced generally near-zero correlations in Table 3, one additional link between the rotated summer AO-like component is noteworthy. Proshutinsky and Johnson (1997) suggest that cyclonic and anticyclonic circulation modes can persist over several years in the Arctic Ocean. They identify anticyclonic ocean circulation regimes from 1946–1952, 1958–1963, 1972–1979, and 1984–1988, while cyclonic regimes dominate from 1953–1957, 1964–1971, 1980–1983 and 1989–1997. Mean values of the NAO and AO scores, obtained from the SLP RPCA analyses, were obtained for the 26 anticyclonic and cyclonic years and the differences between them were tested for statistical significance using a two-tailed *t*-test (Table 4). The same was done for the TW98s SLP scores averaging June–August values to obtain a seasonal mean. RPCA NAO score differences (not shown) were not significant. Table 4 differences in the summer AO scores are, however, highly significant (greater than 99.99% confidence). Positive RPCA AO scores (representing a dominant Arctic anticyclone in the SLP field; e.g., Fig. 4c) occurred in 21 of the 26 anticyclonic ocean circulation years, while 20 of the 26 cyclonic ocean circulation years exhibited negative summer AO scores (mean cyclone akin to Fig. 4d) in our analysis. The NAO/AO mean differences from TW98 are also significant but are near the lower limit for statistical significance with 95% confidence. The results suggest that a rotated summer AO index better represents the circulation of the underlying ocean than the TW98 time series that is mixed with, or "contaminated" by, the NAO.

Because other applications such as Table 4 may exist, the "NAO-free" AO scores for spring, summer and autumn are tabulated in Table 5. Non-winter time series of an "AO-free" NAO remain best represented by the NAO station index used here (Rogers 1984), with its Azores center located close to the warm-season subtropical anticyclone position.

4 Discussion

This study suggests that the existence of a Northern Hemisphere annular mode incorporating the NAO into

Table 5. The RPCA-based AO-like mode's temporal scores (multiplied by 100) during the three seasons when it is separable from the NAO

Year	Spring	Summer	Autumn
1946	1	74	–41
1947	–23	52	82
1948	–95	20	–43
1949	–51	30	–13
1950	–17	58	6
1951	40	9	–70
1952	52	9	44
1953	–75	–46	–13
1954	–48	–106	13
1955	79	–69	–22
1956	–11	–31	37
1957	–5	–17	58
1958	63	–54	–13
1959	–65	94	95
1960	72	99	0
1961	26	124	–62
1962	–11	17	5
1963	–21	26	–37
1964	–29	–12	58
1965	–39	32	–1
1966	98	–36	–68
1967	–69	73	–85
1968	–91	–70	101
1969	–9	39	5
1970	72	–60	–10
1971	–3	–4	–89
1972	33	85	111
1973	40	–59	–50
1974	–25	16	79
1975	–23	33	–71
1976	53	–65	17
1977	–20	95	32
1978	56	99	–37
1979	150	80	28
1980	94	–67	15
1981	–36	31	102
1982	35	–11	70
1983	97	–81	–32
1984	–16	64	87
1985	13	98	32
1986	–15	–3	0
1987	49	66	15
1988	35	–5	–87
1989	7	–193	–33
1990	–228	81	23
1991	–62	–38	–48
1992	–24	–143	54
1993	–31	51	–48
1994	46	–157	–105
1995	14	–89	–85
1996	–53	–61	54
1997	–30	–79	–59

its spatial structure may mainly be a function, at least in non-winter seasons, of one's choice of analytical methodology. An AO-like RPCA pattern, exhibiting a strong SLP response over the Arctic Ocean basin with a weaker mid-latitude response, appears here as an atmospheric low-frequency variability teleconnection pattern separable from the NAO during non-winter seasons (Figs. 1b, 2b, 3b). Our analysis differs from that of Thompson and Wallace (1998, 2000) who maximized dataset variance in their leading EOF, producing a mixed NAO/AO mode in annually stratified and cold-season SLP datasets. The analysis done here redistributes seasonal dataset variance in order to identify the dominant spatial modes of variability, an objective that has been the focus of a variety of studies (e.g., Hsu and Wallace 1985; Barnston and Livezey 1987).

A compelling question from this study is why the NAO and AO might remain inseparable in winter. Hartmann et al. (2000) and Shindell et al. (2001) suggest that the NAO/AO annular mode variability may be related to human influences on stratospheric ozone and/or greenhouse gas concentrations. We suggest here the possibility that the extreme northeastern Atlantic and the Arctic basin share a common storm track during winter, a situation that may not occur as extensively in the non-winter seasons. Rogers (1997) shows that the primary rotated mode of high frequency synoptic-scale (2–8 day periods) SLP variability in winter is not centered over the Denmark Strait, where the long-term mean Icelandic low is found on monthly and seasonal mean charts (e.g., Fig. 4b). Instead the focus of synoptic variability lies over the region northeast of Iceland extending toward the Norwegian and Barents seas. On interannual time-scales, this indicates high variability in the frequency, and intensity, of cyclones migrating into the arctic basin northeast of Iceland. This may not occur during the bulk of spring, summer and autumn months. Indeed, Serreze (1995) and Serreze and Barry (1988) show that the arctic basin has a summer storm track completely disassociated from the NAO with few storms seasonally entering the arctic basin from the northeastern Atlantic. The summer Arctic storm track instead is very active in the baroclinic zone along the Arctic coast in the Laptev and East Siberian seas (Serreze 1995), culminating in high cyclone frequencies over the central Arctic basin at the highest latitudes. The interannual variability in high Arctic summer storminess along this track and orientation is suggestively similar to the pattern of high mean pressure variability shown here in Fig. 2b. The results shown in Table 4 attest to the potential linkages of the summertime AO, and the NAOs lack thereof, to the Arctic Ocean. Systematic analyses of high-frequency pressure variability in non-winter seasons, and even in winter at the highest latitudes, need to be further evaluated.

5 Conclusions

A RPCA has been performed on the seasonal mean SLP anomalies over the Northern Hemisphere. Previous Arctic-inclusive unrotated eigenvector analyses have suggested that the leading mode explaining the greatest dataset variance is one in which the Arctic Oscillation and North Atlantic Oscillation form an annular mode of the hemispheric atmospheric circulation. RPCA is used here to best identify the simple, unique, statistically robust patterns of spatial variability in the SLP dataset, rather than emphasizing a maximization of dataset

variance. It is shown that the NAO and AO appear as separate regional teleconnections when RPCA is performed on spring, summer and autumn data. If the RPCA-based AO pattern represents an annular mode in these seasons, its main center of action is highly confined to the Eurasian side of the Arctic Ocean basin and would be spatially separate from the NAO. During winter however, a distinct AO-like pattern is not obtained using RPCA, and the NAO and AO are arguably inseparable; a result also occurring in an annual analysis incorporating all the monthly data used here from March 1946–February 1998. This is in keeping with the Thompson and Wallace (1998, 2000) analyses although we speculate that the winter NAO and AO are possibly linked by a shared winter storm track across the Norwegian Sea between the northern Atlantic and Arctic basin. Data analyses have yet to adequately address intricacies of the role of seasonal high-frequency pressure variability and storm tracks in Atlantic–Arctic low-frequency teleconnections.

We also demonstrate that the non-winter, separate, AO-like pattern is an important concept for climate diagnosis. The RPCA based AO is correlated to north-central seasonal Siberian and Eurasian air temperatures. The mode (anticyclonic, cyclonic) of the summer RPCA-based AO is also highly related to the direction of rotation of the Arctic Ocean as determined by Proshutinsky and Johnson (1997). This study shows that the AO and NAO are readily separable in non-winter seasons and that climate diagnostics of NAO and AO impacts in those seasons can be made individually, each without a contribution from the other teleconnection.

Acknowledgements This work is partly supported by the National Science Foundation Office of Polar Programs under grant NSF-OPP-9726417. We thank the two anonymous reviewers for their valuable suggestions on improving the manuscript.

References

Barnston AG, Livezey RE (1987) Classification, seasonality and persistence of lowfrequency atmospheric circulation patterns. Mon Weather Rev 115: 1083–1126

Bretherton CS, Smith C, Wallace JM (1992) An intercomparison of methods for finding coupled patterns in climate data. J Clim 5: 541–560

Deser C (2000) On the teleconnectivity of the "Arctic Oscillation". Geophys Res Lett 27: 779–782

Gates WL (1950) A statistical analysis of Northern Hemisphere sea-level pressure patterns accompanying high and low pressure deficit. Bachelor of Science Thesis, Massachuselts Institute of Technology, mass., USA, (unpublished)

Hartmann DL, Wallace JM, Limpasuvan V, Thompson DWJ, Holton JR (2000) Can ozone depletion and global warming interact to produce rapid climate change? Proc Nat Acad Sci 97: 1412–1417

Horel JD (1981) A rotated principal component analysis of the interannual variability of the Northern Hemisphere 500 mb height field. Mon Weather Rev 109: 2080–2092

Horel JD (1984) Complex principal components analysis: theory and examples. J Clim Appl Meteorol 23: 1660–1673

Hsu H, Wallace JM (1985) Vertical structure of wintertime teleconnection patterns. J Atmos Sci 42: 1693–1710

Kutzbach JE (1967) Empirical eigenvectors of sea level pressure, surface temperature and precipitation complexes over North America. J Appl Meteorol 6: 791–802

Kutzbach JE (1970) Large-scale features of monthly mean Northern Hemisphere anomaly maps of sea-level pressure. Mon Weather Rev 98: 708–716

Kushnir Y, Wallace JM (1989) Low-frequency variability in the Northern Hemisphere winter: geographical distribution, structure and time-scale dependence. J Atmos Sci 46: 3122–3142

Metz W (1989) Low-frequency anomalies of atmospheric flow and the effects of cyclone-scale eddies: a canonical correlation analysis. J Atmos Sci 46: 1026–1041

Monahan AH (2000) Nonlinear principal component analysis by neural networks: theory and application to the Lorenz system. J Clim 13: 821–835

Monahan AH, Pandolfo L, Fyfe JC (2001) The preferred structure of variability of the Northern Hemisphere atmospheric circulation. Geophys Res Lett 28: 1019–1022

Namias J (1950) The index cycle and its role in the general circulation. J Meteorol 7: 130–139

Nicholls N (1987) The use of canonical correlation to study teleconnections. Mon Weather Rev 115: 393–399

O'Lenic EA, Livezey RE (1988) Practical considerations in the use of rotated principal component analysis (RPCA) in diagnostic studies of upper-air height fields. Mon Weather Rev 116: 1682–1689

Proshutinsky AY, Johnson MA (1997) Two circulation regimes of the wind-driven Arctic Ocean. J Geophys Res 102: 12,493–12,514

Richman MB (1986) Rotation of principal components. J Climatol 6: 293–335

Richman MB (1987) Rotation of principal components: a reply. J Climatol 7: 511–520

Rogers JC (1984) The association between the North Atlantic Oscillation and the Southern Oscillation in the Northern Hemisphere. Mon Weather Rev 112: 1999–2015

Rogers JC (1990) Patterns of low-frequency monthly sea level pressure variability (1899–1986) and associated wave cyclone frequencies. J Clim 3: 1364–1379

Rogers JC (1997) North Atlantic storm track variability and its association to the North Atlantic Oscillation and climate variability of Northern Europe. J Clim 10: 1635–1647

Rogers JC, van Loon H (1982) Spatial variability of sea level pressure and 500 mb height anomalies over the Southern Hemisphere. Mon Weather Rev 110: 1375–1392

Rogers JC, Mosley-Thompson E (1995) Atlantic Arctic cyclones and the mild Siberian winters of the 1980s. Geophys Res Lett 22: 799–802

Serreze MC (1995) Climatological aspects of cyclone development and decay in the Arctic. Atmos-Ocean 33: 1–23

Serreze MC, Barry RG (1988) Synoptic activity in the Arctic basin, 1979–85. J Clim 1: 1276–1295

Shindell DT, Schmidt GA, Miller RL, Rind D (2001) Northern Hemisphere winter climate response to greenhouse gas, ozone, solar, and volcanic forcing. J Geophys Res 106: 7193–7210

Thompson DWJ, Wallace JM (1998) The Arctic Oscillation signature in the wintertime geopotential height and temperature fields. Geophys Res Lett 25: 1297–1300

Thompson DWJ, Wallace JM (2000) Annular modes in the extratropical circulation. Part I: month-to-month variability. J Clim 13: 1000–1016

Trenberth KE, Paolino DA (1980) The Northern Hemisphere sea level pressure data set: trends, errors and discontinuities. Mon Weather Rev 108: 855–872

Trenberth KE, Paolino DA (1981) Characteristic patterns of variability of sea level pressure in the Northern Hemisphere. Mon Weather Rev 109: 1169–1189

van Loon H, Rogers JC (1978) The seesaw in winter temperatures between Greenland and northern Europe. Part I: general description. Mon Weather Rev 106: 296–310

Walker GT, Bliss EW (1932) World Weather V. Mem R Meteorol Soc 44: 53–84

Wallace JM (2000) North Atlantic Oscillation/annular mode: two paradigms – one phenomenon. Q J R Meteorol Soc 126: 791–805

Wallace JM, Gutzler DM (1981) Teleconnections in the geopotential height field during the Northern Hemisphere winter. Mon Weather Rev 109: 784–812

Wallace JM, Smith C, Bretherton CS (1992) Singular value decomposition of wintertime sea surface temperature and 500-mb height anomalies. J Clim 5: 561–576

Walsh JE, Richman MB (1981) Seasonality in the associations between surface temperature over the United States and the North Pacific Ocean. Mon Weather Rev 109: 767–783